Environ Earth Sci (2015) 74:5949–5959
DOI 10.1007/s12665-015-4618-x

ORIGINAL ARTICLE

Projecting the dynamics of terrestrial net primary productivity in response to future climate change under the RCP2.6 scenario

Chengcheng Gang[1,2,3] · Zhaoqi Wang[3] · Wei Zhou[4] · Yizhao Chen[3] · Jianlong Li[3] · Jimin Cheng[1,2] · Liang Guo[1,2] · Inakwu Odeh[5] · Chun Chen[4]

Received: 21 July 2014 / Accepted: 7 June 2015 / Published online: 2 July 2015

Abstract This paper aims to reveal the responses of global natural vegetation to future climate change in the twenty-first century. Thus, the dynamics of terrestrial net primary productivity (NPP) in three time slices, namely, 2030s, 2050s and 2070s are projected using a segmentation model that utilized 25 global climate models under the Representative Concentration Pathway 2.6 (RCP2.6) scenario. The results showed that forests would expand at the expense of grasslands and deserts in the current century. Terrestrial NPP is projected to increase globally from 127.04 ± 1.74 Pg DW·a^{-1} in 2030s to 127.62 ± 2.57 Pg DW·a^{-1} in 2070s. Temperate forest, the largest distributed vegetation, would contribute the most to the overall increase (548.50 Tg DW·a^{-1}). The NPP of warm desert, savanna, and tropical forest is projected to increase by 31.03, 248.45 and 111.25 Tg DW·a^{-1}, respectively. By contrast, the NPP of all the other vegetations would decline at the end of this century. In the tropical and the south temperate zones, terrestrial NPP is projected to decrease by 99.32 and 25.56 Tg DW·a^{-1}, respectively, with the difference lying in the increasing–decreasing trend in the former and the continually decreasing trend in the latter. However, terrestrial NPP in the north temperate and north frigid zones is projected to increase consistently by 639.43 and 57.73 Tg DW·a^{-1}, respectively. The "increase-peak-decline" trend of greenhouses gases described in the RCP2.6 would lead to the warming and cooling periods during this century. The vegetation NPP of various ecosystems or climate zones would respond differently to the future climate change. In general, ecosystems in northern high latitudes would become more vulnerable to future climate change compared to other vegetations.

Keywords Comprehensive sequential classification system (CSCS) · Representative concentration pathway (RCP2.6) · Multi-model ensemble mean (MME) · Potential natural vegetation (PNV) · Net primary productivity (NPP)

✉ Jianlong Li
jianlongli@gmail.com

[1] Institute of Soil and Water Conservation, Northwest A&F University, Yangling 712100, People's Republic of China

[2] Institute of Soil and Water Conservation, Chinese Academy of Science and Ministry of Water Resources, Yangling 712100, People's Republic of China

[3] The Global Change Research Institute, School of Life Sciences, Nanjing University, No. 22 Hankou Road, Nanjing 210093, People's Republic of China

[4] School of Architecture and Urban Planning, Chongqing Jiaotong University, Chongqing 400074, People's Republic of China

[5] Department of Environmental Science, Faculty of Agricultural and Environment, The University of Sydney, Sydney 2006, Australia

Introduction

The recognition of the interactions between terrestrial ecosystems and climate change is crucial in global change research. Numerous studies have focused on the effects of climate change on terrestrial ecosystems, as well as on their feedbacks (Nemani et al. 2003; Melillo et al. 1993; Cao and Woodward 1998). Climate is a factor of long-term, primary importance in determining terrestrial ecosystems and their distributions with vegetation is the most direct reflection (Zhang 1993). Precipitation and temperature, which control the evaporation rate of natural ecosystems, further impact the photosynthesis process and content of soil organic matters, and finally influence the material and energy flows

of ecosystems. They are the prominent factors that affect vegetation (Foley et al. 2000; Horion et al. 2013). In the last century, increased evidence became available from a wider range of species and communities in terrestrial ecosystems indicating that recent warming is strongly affecting terrestrial ecosystem structures and functions (Canadell et al. 2006; Gang et al. 2013; Parton et al. 1995; Gao et al. 2013). Current studies on regional and global climate effects on terrestrial ecosystems reveal consistent responses to the warming trend. The research timescales ranged from decadal to century, and the spatial scales cover regions and the globe (Ren et al. 2011a, b; Gao et al. 2013; Motew and Kucharik 2013; Piao et al. 2011; Grimm et al. 2013). According to the latest Fifth Assessment Report of Intergovernmental Panel on Climate Change (IPCC 5AR), the warming trend would continue during this century, such that impacts are expected to increase and perhaps even accelerate (IPCC 2012). Therefore, evaluating the effect of future climate change on terrestrial ecosystems is essential.

A new set of scenarios, the Representative Concentration Pathways (RCPs), are conducted in the IPCC 5AR under the framework of the Coupled Model Intercomparison Project Phase 5 (CMIP5) of the World Climate Research Programme (IPCC 2012). The climate change from the RCP scenarios is framed as a combination of the adaptation and mitigation as compared with the 4AR. The comprehensive climate models involved produce a range of responses to the ongoing warming. The RCP2.6 is a stringent mitigation scenario that describes a future world with an increased global mean temperature of less than 2 °C, cumulative emissions of greenhouse gases that would peak in 2050s and then decline moderately, which would be reduced by 70 % by 2100 compared with the baseline scenario assuming the full participation of all countries (Van Vuuren et al. 2011a, b). The effects of future climate change on terrestrial ecosystems are currently, substantially studied (Anav and Mariotti 2011; Hickler et al. 2012; Lenihan et al. 2003; Alo and Wang 2008). However, most of these studies mainly focused on the regional scale, and the process and extent in which terrestrial vegetation would be impacted by future climate change under the state-of-the-art scenarios at the global scale are reported less. Therefore, considering the possible terrestrial vegetation responses induced by future climate changes is necessary to fill in this gap.

Observed changes in several physical and biological systems demonstrated the consistent responses to warming trends, including high latitude/elevation shifts of tundra species and lengthy growth seasons (Gang et al. 2013; Woodward 1987; Menzel and Fabian 1999). The responses of different ecosystems to climate change varied in terms of species and regions. Changes in the abundance of certain species, including limited evidences on a few local disappearances, and changes in community composition over the past few decades, were attributed to climate change (Pearson and Dawson 2003; Marshall et al. 2010; Massot et al. 2008). The concept of potential natural vegetation (PNV) was frequently used to distinguish the responses of different ecosystems to climate change. Numerous studies were conducted to reconstruct the past or project the future vegetation since its introduction (Hickler et al. 2012; Brzeziecki et al. 1995; Yue et al. 2011; Gonzalez et al. 2010). This study utilized the modified Comprehensive Sequential Classification System (CSCS) to project global vegetation maps under future climate conditions. The CSCS was established based on the relationships of climate, soil, and vegetation, and mainly driven by mean temperature and precipitation. This system was successfully used in simulating terrestrial vegetation at various scales (Gang et al. 2013; Ren et al. 2008, 2011).

Net primary productivity (NPP) refers to the organic matters fixed by plants in photosynthesis, which provides a link between the biomes and the climate system through the global carbon and water cycles (Odum 1976). NPP can indicate the plant growth ability in a specific natural environment. Thus, its dynamics can reflect ecosystem variations in response to climate change (Roy et al. 2001; Cao et al. 2005). To date, research on terrestrial NPP at various levels has increased significantly. NPP estimation models, such as climate-based models (i.e. Miami model (Lieth 1977), Thornthwaite Memorial model (Lieth and Eas 1972), process-based models (i.e. CENTURY (Parton et al. 1993), TEM (Mcguire et al. 1995), BIOME-BGC (Running and Hunt 1993) as well as light use efficiency models [i.e. CASA (Potter et al. 1993); GLO-PEM (Prince 1991)], are widely reported. However, process-based models require many complicated parameters, which render it superior in estimating local NPP. By contrast, light use efficiency models are much more widely used in regional or global NPP estimations because of the readily accessible information from remote sensing data. However, the satellite-based parameters used in these models, i.e. normalized difference vegetation index, are only accessible in the last 30 years, which prevents century-long application. The climate-based models are valuable and capable in detecting vegetation NPP and their variations in response to climate change (Zhu et al. 2005). This paper uses a segmentation model based on actual evapotranspiration and photosynthesis of vegetation to evaluate terrestrial NPP and their variations in response to future climate change.

Climate change across the globe clearly causes severe ecological and environment problems, with a notable increase in extreme climate event frequencies. Changes in

the large-scale distribution and productivity of terrestrial ecosystems are associated with climate change in different manners. One of the challenges in global change research is identifying the extent in which future climate change would affect the terrestrial ecosystems. To better clarify this issue, the terrestrial NPP dynamics across three time slices, namely, 2030s, 2050s, and 2070s, are projected based on 25 General Circulation Models (GCMs) under the RCP2.6 scenario. The outcomes of this study do not only provide a general outlook of the responses of terrestrial ecosystems to upcoming decades of climate change, but may also partly complement the IPCC report. Furthermore, the methods used in this paper can serve as a guidance for regions lacking of collected/observed data.

Materials and methods

Global climatic data

The CMIP5 features substantial model improvements compared to CMIP3 and utilizes a new set of emission scenarios which is known as RCPs. In this paper, a set of the global climate data from 25 GCMs under the RCP2.6 scenario were used as input data in the CSCS to generate global PNV maps, and in the segmentation model to simulate terrestrial NPP. These GCMs were obtained from the International Center for Tropical Agriculture climate change portal (http://ccafs-climate.org/data) at a 2.5 arc-minute resolution (~5 km), which was provided and pre-processed by the Tyndall institute. The information of 25 GCMs is listed in Table 1. The mean annual temperature (MAT) and mean annual precipitation (MAP) data in three time intervals, namely, 2030s, 2050s, and 2070s were incorporated from monthly gridded data using the ArcGIS v10.1 software.

The modified CSCS model

Based on the water and thermal conditions, the CSCS model is composed of three levels: class, subclass, and type (Liang et al. 2012; Ren et al. 2008). The class level, the basic unit, is determined by bioclimatic conditions, the subclass level is classified by edaphic conditions, and the type level is based on vegetation characteristics. Subclasses are integrated into classes according to an index of moisture and temperature which reflects the natural occurrence of vegetation ecosystems. The classes are mainly established by the humidity index (K), a function of MAP and annual cumulative temperature above 0 °C ($\Sigma\theta$) (Growing Degree Days on 0 °C base, GDD0). It is expressed as:

$$K = \mathrm{MAP}/(0.1 \times \Sigma\theta) = \mathrm{MAP}/(0.1 \times \mathrm{GDD0}) \quad (1)$$

where MAP is the mean annual precipitation (mm) and 0.1 is an empirical parameter. The original version of CSCS documents 42 classes. In this study, the system was further improved, in which the Polar/Nival type was identified (Fig. 1). To more explicitly reflect the spatial distribution of PNV at the global scale, classes were regrouped into 11 vegetation types, i.e. polar/nival, tundra & alpine steppe, cold desert, semi-desert, steppe, temperate humid grassland, warm desert, savanna, temperate forest, subtropical forest, tropical forest. The polar/nival was not discussed in this study.

NPP estimation: the segmentation model

NPP of the natural vegetation was simulated using a segmentation model, which is established according to the humidity index (K) in Eq. 1. The model was established based on actual evapotranspiration, which is closely related to the photosynthesis of vegetation (Zhou et al. 1998; Zhang et al. 2011; Uchijima and Seino 1985). This model integrated the interaction among many variables, and was expressed as follows:

$$\mathrm{NPP} = \begin{cases} \dfrac{\mathrm{RDI} \times \mathrm{MAP} \times R_n \times \left(\mathrm{MAP}^2 + R_n^2 + \mathrm{MAP} \times R_n\right)}{(\mathrm{MAP} + R_n)(\mathrm{MAP}^2 + R_n^2)} \\ \times \exp\left[-\sqrt{(9.87 + 6.25RDI)}\right] \times 100 \quad (K < 1.2) \\ 0.29\exp(-0.216RDI^2) \times R_n \qquad (K > 1.2) \end{cases} \quad (2)$$

$$\mathrm{RDI} = 0.629 + 0.237\ \mathrm{PER} - 0.00313\ \mathrm{PER}^2 \quad (3)$$

$$R_n = \mathrm{RDI} \times \mathrm{MAP} \times L \times 2.38 \times 10^{-4} \quad (4)$$

$$\mathrm{PER} = \mathrm{PET}/MAP = 1.6145/K \quad (5)$$

where MAP is the mean annual precipitation (mm), RDI is radioactive dryness index which can be calculated by PER, PER is the rate of evapotranspiration, R_n is the intercepted net radiation ($\mathrm{J \cdot cm^{-1} \cdot a^{-1}}$), L is latent heat (2503 $\mathrm{J \cdot g^{-1}}$), PET is potential evapotranspiration (mm), K is humidity index calculated by Eq. 1. NPP is calculated in unit of g $\mathrm{DW \cdot m^{-2} \cdot a^{-1}}$.

The modelled NPP results have been validated using the Global Primary Production Data Initiative dataset, which includes 5164 sites that represent the majority of global biomes (Olson et al. 2012). The validation results showed that the modelled NPP results are in well agreement with field NPP data from different biomes (Fig. 2).

Table 1 The information of 25 GCMs under the RCP2.6 scenario

GCMs	Modelling group	Country
bcc_csm1_1	The Beijing Climate Center Climate model	China
bcc_csm1_1_m		
bnu_esm	Beijing Normal University - Earth System Model	
fio_esm	The First Institute of Oceanography-Earth System Model	
lasg_fgoals_g2	Institute of Atmospheric Physics, Chinese Academy of Sciences	
cccma_canesm2	The Coupled Global Climate Model, Canadian Centre for Climate Modelling and Analysis	Canada
csiro_mk3_6_0	The Commonwealth Scientific and Industrial Research Organization	Australia
cesm1_cam5	The Community Earth System Model, Community Atmosphere Model	U.S.A.
gfdl_cm3	The Geophysical Fluid Dynamic Laboratory	
gfdl_esm2 g		
gfdl_esm2 m		
giss_e2_h	NASA Goddard Institute for Space Studies	
giss_e2_r		
ncar_ccsm4	The National Center for Atmospheric Research	
ipsl_cm5a_lr	The Institute Pierre et Simon Laplace	France
ipsl_cm5a_mr		
mri_cgcm3	Meteorological Research Institute	Japan
miroc_esm	Japan Agency for Marine-Earth Science and Technology, Atmosphere and Ocean Research Institute	
miroc_esm_chem		
miroc_miroc5	Atmosphere and Ocean Research Institute, National Institute for Environmental Studies, and Japan Agency for Marine-Earth Science and Technology	
mohc_hadgem2	Met Office Hadley Centre	U.K.
mpi_esm_lr	The Max Planck Institute for Meteorology coupled climate model	Germany
mpi_esm_mr		
ncc_noresm1_m	Norwegian Climate Centre	Norway
nimr_hadgem2_ao	National Institute of Meteorological Research/Korea Meteorological Administration	Korea

Results

Future climate change in this century

Projected MAT and MAP anomalies in 2070s relative to 2030s are shown in Fig. 3. The multi-model ensemble mean (MME) results indicated an increase in the MAT with an average of 0.168 °C at the end of this century. The maximum increase is predicted at 0.770 °C by the gfdl_cm3, in which the positive trend of MAT would transpire across the globe, whereas the minimum increase is projected at 0.034 °C by the bnu_esm. The decreasing trend of MAT is projected across five GCMs. Regions presenting an increasing MAT trend on the average would amount to 70.78 % of total lands during this century. The MME results showed that MAP would increase globally with 3.939 mm, such that 53.59 % of regions would experience averagely increasing MAP. The MAP dynamic would present obvious spatial heterogeneity, particularly in tropical regions. In general, most GCMs predicted that the future world would become increasingly warm and wet at the end of this century.

Natural vegetation responses to future climate change

Areas of ten PNV units in 2030s, 2050s, and 2070s were projected using the modified CSCS (Table 2). The results showed that during this century, forests would expand at the expense of grasslands and deserts. The area of the forest is projected to increase by 36.82×10^4 km^2, in which temperate forest, the most widely distributed vegetation, would increase the most. Distributions of subtropical and tropical forests would shrink by 1.17 %. Grassland ecosystems are projected to decrease averagely by 0.73 %. Among the four grassland types, only savanna is projected to expand by 1.08 %, the areas of tundra & alpine steppe, as well as that of steppe and temperate humid grassland would decrease by 4.04, 1.67 and 1.35 %, respectively. Deserts, the least distributed vegetation, are also projected to decrease by

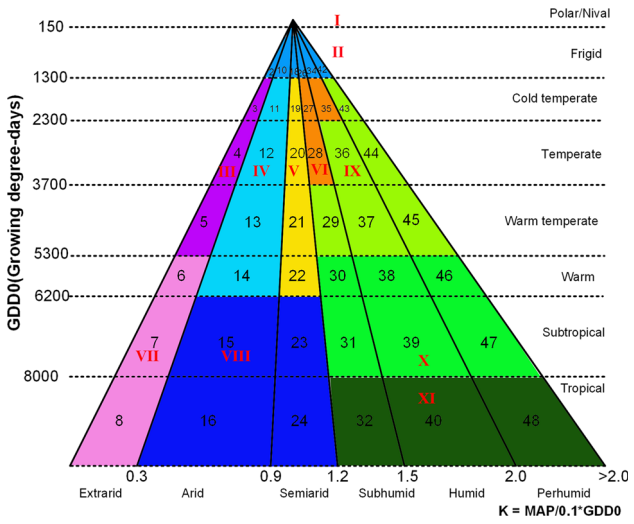

Fig. 1 The index chart of the modified CSCS. The modified CSCS documents 48 classes. To more explicitly visualize the distribution and variation of PNV at the global scale, 48 classes were combined into 11 PNV units: I: Polar/Nival; II: Tundra &alpine steppe; III: Cold desert; VI: Semi-desert; V: Steppe; VI: Temperate humid grassland; VII: Warm desert; VIII: Savanna; IX: Temperate forest; X: Subtropical forest XI: Tropical forest

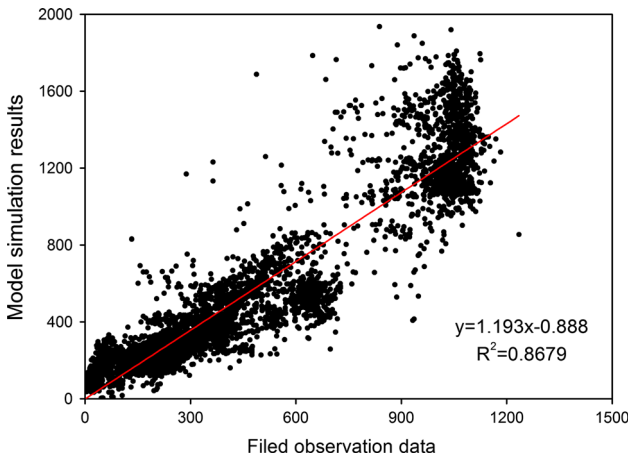

Fig. 2 Comparison of modelled NPP value and observed data ($p < 0.001$). The observed data are collected from the Oak Ridge National Laboratory (ORNL). These data, and further information about the study sites, are publicly available at www.daac.ornl.gov/NPP/

0.35 % averagely. The area of warm desert would expand by 1.00 %. By contrast, the areas of cold desert and semi-desert would decrease by 5.10 and 2.59 %, respectively.

Terrestrial NPP responses to future climate change

Terrestrial NPP and their dynamics during this century were projected using the segmentation model (Fig. 4). The results showed that global terrestrial NPP would increase from 127.04 ± 1.74 Pg DW·a^{-1} in 2030s to 127.62 ± 2.57 Pg DW·a^{-1} in 2070s.

At the global scale, the NPP of temperate forest is projected to averagely increase the most by 548.50 Tg DW·a^{-1}. The increasing trend in 2030s–2050s would amount to 354.15 Tg DW·a^{-1}. Warm desert NPP would similarly increase continuously in this century with a rate of 31.03 Tg DW·a^{-1}. Tropical forest and savanna NPP are projected to increase by 111.25 and 248.45 Tg DW·a^{-1}, respectively. Both of their NPP would share the same changing trends with increases in 2030s–2050s, and decreases in 2050s–2070s. Steppe NPP would present the same pattern with an overall decrease of 21.91 Tg DW·a^{-1} in 2070s relative to 2030s. The NPP of tundra & alpine steppe, cold desert, temperate humid grassland and subtropical forest is projected to decrease by 137.29, 3.14, 15.41 and 125.39 Tg DW·a^{-1} at the end of this century, respectively. All their NPP would decrease obviously from 2030s to 2050s, and increase slightly thereafter. In addition, semi-desert NPP is projected to decline continuously by 52.65 Tg DW·a^{-1} during this century.

From the perspective of climatic zones, the NPP in the tropical zone (TRZ), which accounts for nearly 60 % of the total terrestrial NPP, is projected to decrease from 72904.76 ± 1218.65 Tg DW·a^{-1} in 2030s to 72805.44 ± 1526.02 Tg DW·a^{-1} in 2070s (Fig. 5). The largest increase would be in savanna, which is projected to increase continuously by 201.43 Tg DW·a^{-1}. Similarly, warm desert NPP would increase by 14.59 Tg DW·a^{-1}. Cold desert NPP is projected to increase slightly with a rate of 0.02 Tg DW·a^{-1}. By contrast, the NPP of all the other vegetations is projected to decrease at the end of this century. Tropical forest NPP, which amounts to over 75 % of the total NPP in the TRZ, is projected to decrease by 46.67 Tg DW·a^{-1}. Most of the decrease of 261.49 Tg DW·a^{-1} would occur in subtropical forest. The NPP of the north frigid zone (NFZ) is projected to increase from 2264.79 ± 177.10 Tg DW·a^{-1} in 2030s to 2322.52 ± 254.10 Tg DW·a^{-1} in 2070s. Most of the increase would be attributed to the temperate forest, whose NPP is projected to increase by 67.41 Tg DW·a^{-1}. An increasing trend is projected in temperate humid grassland as well. The NPP of tundra & alpine steppe, which accounts for nearly 70 % of the total NPP in the NFZ, is projected to decrease by 20.53 Tg DW·a^{-1}. The NPP in the north temperate zone (NTZ) is projected to increase continuously by 639.43 Tg DW·a^{-1} and temperate forest would contribute the most by 494.16 Tg DW·a^{-1}. The NPP of subtropical and tropical forests would increase by 181.29 and 111.87 Tg DW·a^{-1}, respectively. Similarly, ascending trends are also projected in warm desert and savanna, by 7.20 and 36.96 Tg DW·a^{-1}, respectively. However, the NPP in higher

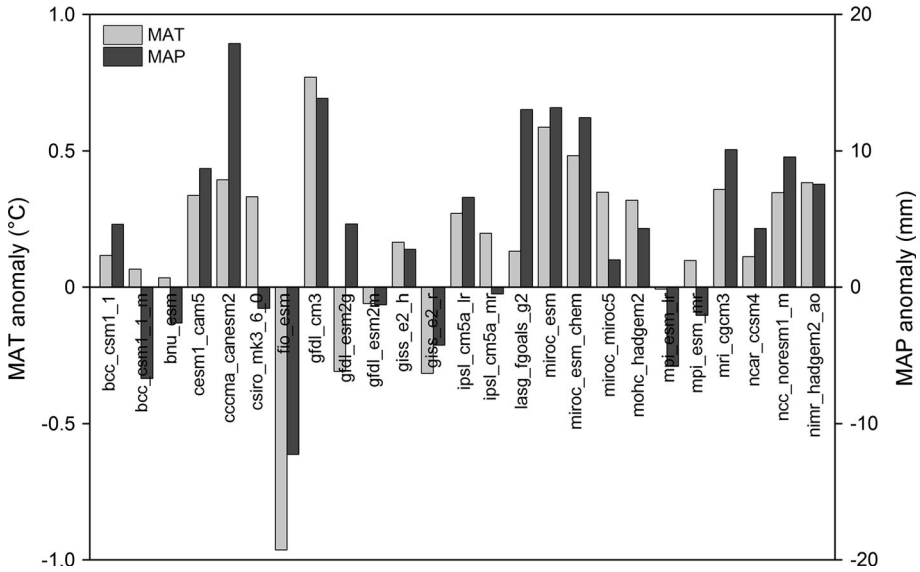

Fig. 3 The projected anomalies of MAT and MAP in 2070s relative to 2030s based on 25 GCMs under the RCP2.6 scenario

Table 2 The area of each terrestrial ecosystem in 2030s, 2050s, and 2070s under the RCP2.6 scenario. (Unit: $\times 10^4$ km^2)

	2030s	2050s	2070s
Tundra & alpine steppe	1048.04 ± 148.08	1001.77 ± 176.70	1005.71 ± 198.00
Cold desert	170.50 ± 32.04	161.87 ± 32.43	161.80 ± 34.58
Semi-desert	742.22 ± 26.66	732.66 ± 33.84	723.00 ± 32.25
Steppe	397.63 ± 24.69	398.12 ± 24.31	391.00 ± 27.21
Temperate humid grassland	388.52 ± 44.84	379.80 ± 49.96	383.25 ± 47.95
Warm desert	1824.79 ± 85.23	1844.59 ± 96.76	1843.00 ± 96.24
Savanna	2242.64 ± 85.94	2271.03 ± 112.51	2266.93 ± 122.26
Temperate forest	3037.28 ± 134.42	3067.69 ± 166.08	3083.36 ± 183.20
Subtropical forest	861.02 ± 38.22	845.95 ± 39.76	850.93 ± 39.06
Tropical forest	2416.17 ± 52.16	2424.59 ± 54.54	2416.99 ± 60.94

latitudes would present a descending trend. The NPP of tundra & alpine steppe would decrease the most by 111.86 Tg DW·a^{-1}. In the case of the south temperate zone (STZ), NPP in this zone is just one fifth of that in the NTZ owing to the vast ocean area. Terrestrial NPP is predicted to decline continually from 2030s to 2070s by 25.56 Tg DW·a^{-1}. The NPP of warm desert, savanna and tropical forest is projected to increase by 9.14, 9.95 and 38.63 Tg DW·a^{-1}, respectively, at the end of this century, whereas the NPP of all the other vegetations is projected to diminish. The NPP of temperate and subtropical forests is forecasted to decline by 13.95 and 44.80 Tg DW·a^{-1}, respectively. In addition, the NPP of vegetation in higher latitude, including tundra & alpine steppe, cold desert, semi-desert, steppe and temperate humid grassland, is projected to decrease at a rate of 2.08, 0.05, 15.82, 5.93 and 0.61 Tg DW·a^{-1}, respectively. The NPP of each vegetation type in the four climate zones are listed in Table 3.

Discussion

Discussion of the methodology

Natural vegetation maps across the three time slices of this century were simulated using the modified CSCS. The CSCS was constructed by linking vegetation with their climatic and edaphic factors (Ren et al. 2008). This system presents promising applications in simulating vegetation maps due to its readily accessible parameters, especially for regions or periods lacking collected/observed data (Gang et al. 2013). However, it has to be acknowledged that the CSCS failed to incorporate the direct effects of CO_2 fertilization and nitrogen deposits on plant growth and competition. It also did not explicitly include the influence of potential climate-induced changes in disturbance, such as changing incidence of fire and insect outbreaks and pathogens. Furthermore, no assumption on the effects of

Table 3 NPP of each ecosystem and their changing trends in the four climate zones in this century (Unit: Tg DW·a^{-1})

	TRZ*	NFZ	NTZ	STZ
Tundra & alpine steppe	26.08 ± 8.05	1552.46 ± 142.26	2669 ± 579.61	52.67 ± 8.00
	(−10.80 %)	(−1.31 %)	(−4.06 %)	(3.85 %)
Cold desert	2.84 ± 1.45	×	90.79 ± 17.04	11.78 ± 6.67
	(0.69 %)	×	(−3.33 %)	(0.40 %)
Semi-desert	56.09 ± 7.47	×	1928.39 ± 70.81	375.00 ± 46.95
	(−2.23 %)	×	(−1.83 %)	(4.09 %)
Steppe	35.65 ± 7.51	1.09 ± 0.91	1385.47 ± 116.80	155.10 ± 20.13
	(−1.73 %)	(−32.94 %)	(−1.08 %)	(3.70 %)
Temperate humid grassland	11.01 ± 2.89	80.19 ± 54.57	1689.19 ± 181.87	21.64 ± 2.86
	(−1.92 %)	(16.98 %)	(−1.57 %)	(3.70 %)
Warm desert	521.56 ± 71.01	×	408.13 ± 32.27	380.88 ± 42.23
	(2.85 %)	×	(1.79 %)	(−2.76 %)
Savanna	12228.21 ± 490.88	×	2190.67 ± 201.39	2051.00 ± 251.90
	(1.66 %)	×	(1.71 %)	(2.42 %)
Temperate forest	669.79 ± 63.38	604.23 ± 315.64	23404.60 ± 1222.59	1469.27 ± 59.02
	(−0.30 %)	(12.02 %)	(2.14 %)	(−0.94 %)
Subtropical forest	4439.29 ± 582.92	×	6978.52 ± 440.20	2684.31 ± 234.41
	(−5.64 %)	×	(2.64 %)	(−1.65 %)
Tropical forest	54895.40 ± 1429.58	×	1982.30 ± 286.79	613.60 ± 93.03
	(−0.09 %)	×	(5.85 %)	(6.55 %)

× indicates that a type of vegetation would not exit in a continent; a negative sign within parentheses indicates a decreasing trend

* TRZ, the tropical zone; NFZ, the north frigid zone; NTZ, the north temperate zone; STZ, the south temperate zone

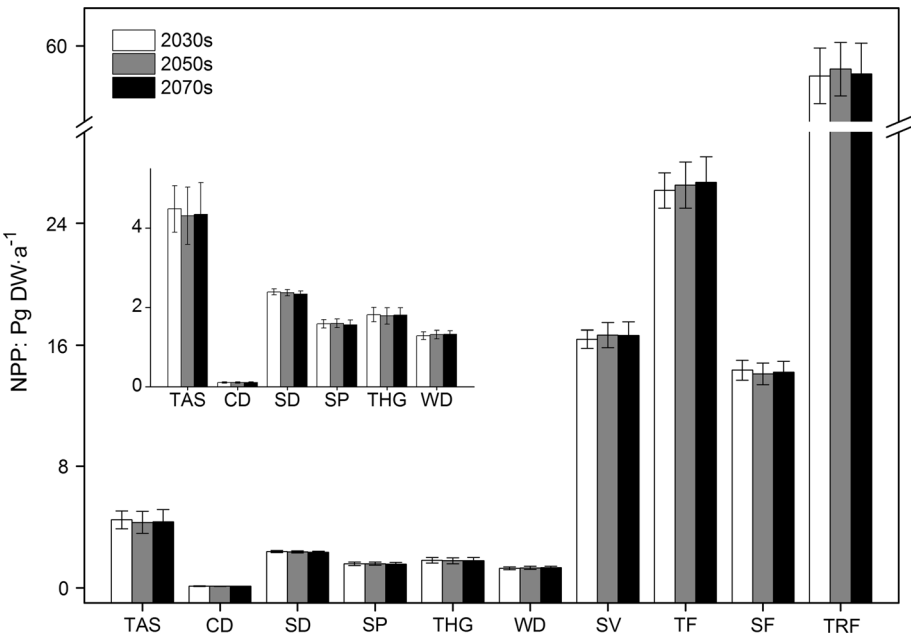

Fig. 4 Dynamics of terrestrial NPP in three time slices 2030s, 2050s, and 2070s. The margin of errors is determined by 25 GCMs under RCP2.6 scenario. The proportion of each vegetation NPP to total terrestrial NPP: 3.44 % for tundra & alpine steppe, 0.08 % for cold desert, 1.86 % for semi-desert, 1.24 % for steppe, 1.41 % for temperate humid grassland, 1.03 % for warm desert, 12.99 % for savanna, 20.77 % for temperate forest, 11.15 % for subtropical forest, 45.98 % for tropical forest

human activities, such as grazing, agricultural development, urbanization, logging, or irrigation, was made in this system. Nevertheless, CSCS enables a novel method of simulating natural vegetation classification because it easily demonstrates the spatial zonal distributions and dynamics of vegetation systems in given specific climate

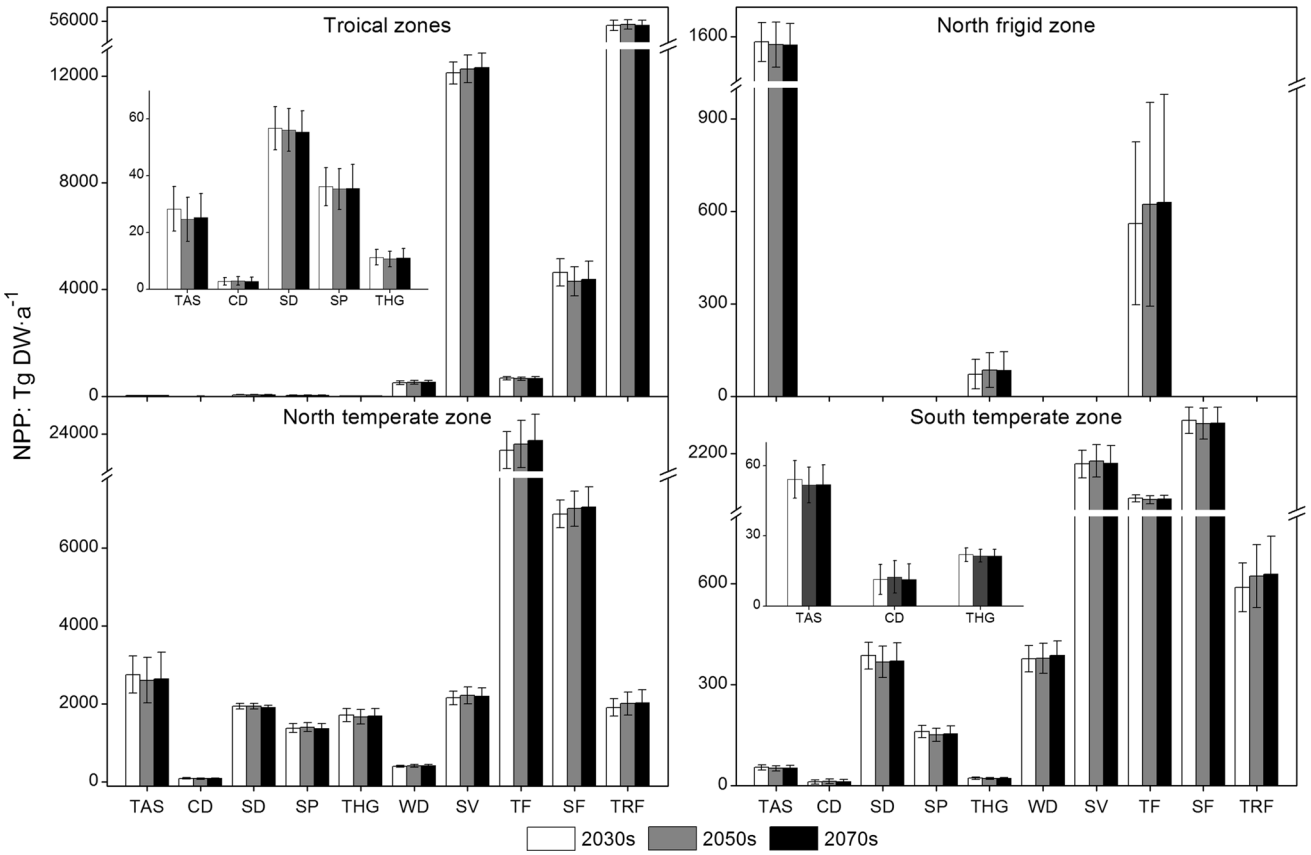

Fig. 5 Dynamics of terrestrial NPP in the four climate zones in three time slices 2030s, 2050s, and 2070s. The margin of errors is determined by 25 GCMs under RCP2.6 scenario. TRZ, the tropical zone; NFZ, the north frigid zone; NTZ, the north temperate zone; STZ, the south temperate zone

conditions at the global scale. Therefore, it is a feasible approach to map the global biomes and their succession associated with global climate change in a span of a century.

MAT and MAP are two primary input parameters used in the modified CSCS and the segmentation model. This study derived these data from the 25 GCMs under the RCP2.6 scenario. Based on the simulation results, five GCMs forecasted a decreasing trend of MAT in the 2070s relative to the 2030s. Although the overall warming trends are projected in most GCMs, uncertainties continue to persist. GCMs are large-scale representations of the atmosphere and its processes. Different physical processes involved in parameterization schemes would cause various GCM sensitivities to radioactive forcing, which leads to the discrepancies in projecting the climate trends in this century among different GCMs (Zhang et al. 2013). Zhang et al. (2013) tested the uncertainties of 29 GCMs of RCP2.6 in projecting the MAT trend of this century. Their reliability analysis results indicated that the warming trends predicted by GCMs in the twenty-first century were credible. The GCMs used in this study were processed using a downscaling method, which was based on the sum of interpolated anomalies to high resolution monthly climate surfaces from WorldClim (Hijmans et al. 2005). This method assumes that changes in climates are only relevant at coarse scales and the relationships between variables are maintained towards the future (Ramirez-Villegas and Jarvis 2010). However, they may not be applicable given the larger errors of highly heterogeneous landscapes with complex topographic conditions. To reduce errors and biased results, this paper utilized all available GCMs instead of selecting a subset of GCMs alone.

Effects of future climate change on terrestrial ecosystems

Concomitant with increasing atmospheric carbon dioxide concentrations, the consistent temperature rises and redistributed rainfall patterns are estimated as major forces that influence ecosystem structures and functions, as well as the geographical ranges of species (IPCC 2007). This study aims to identify better the responses of terrestrial ecosystems to future climate change during the twenty-first century by initially assessing the overall trends of climate variables across the globe, as a basis for subsequently

predicting the likely impacts of these changes on the distributions and variations of terrestrial NPP under the state-of-the-art RCP2.6 scenario. The MME results demonstrated that ecosystems in the northern mid/high latitudes are likely to become features of the responses of natural vegetation to the ongoing climate change.

Terrestrial NPP is projected to increase in this century at a lower rate in 2050s–2070s relative to that in 2030s–2050s. Based on the RCP2.6 description, the greenhouse gases (GHG) concentrations would increase at the first half period of this century, peaking at circa 2050s and decline at the latter half of the century. Accordingly, warming and cooling periods corresponding to the "increase-peak-decline" trend of GHGs would persist. Thus, terrestrial NPP would increase from 2030s to 2050s, and slow down in 2050s to 2070s. In the warming period, the MAT would rise globally, particularly at mid/high latitudes in the northern hemisphere. The precipitation during this warming period is expected to increase prominently in the northern hemisphere. MAP increase would strengthen the intensity of the global warming through the latent heating feedback (Xin et al. 2013; Xu et al. 2005). Based on our results, the NPP of steppe, warm desert, and savanna, as well as temperate and tropical forests would heighten in this period, particularly the savanna in Africa and South America and temperate forest in Asia and North America. The increasing trend of temperate forest NPP had been undertaken in the northern hemisphere from 1901 to 2009 (Wang et al. 2010; Jiang et al. 1999). Furthermore, this trend is in line with basal area measurements, which can be attributed to the collective expansion of distribution areas, increase in growing season lengths, and rise in atmospheric CO_2 concentrations (Lewis et al. 2009; Mcmahon et al. 2010). Temperatures in Africa are projected to rise faster than the global average increase of the twenty-first century, and together with the projected MAP increase over areas of central and eastern Africa at the beginning of twenty-first century would contribute to the increase of savanna NPP (James and Washington 2013; Joshi et al. 2011). However, the rising temperature in this period would lead to the decrease of NPP in other vegetations. The most decreases would transpire in tundra & alpine steppe, particularly in North America and Asia. The responses of terrestrial species to warming across the northern hemisphere are well documented by changes in shifts and dynamics of the vegetation community, including poleward and elevational range shifts of flora and fauna. The wide advancement of temperate forest into the current habitat of tundra would cause the substantial contraction and decline of tundra NPP, which is consistent with findings from other previous studies (Cramer et al. 2001; Gang et al. 2013; Lucht et al. 2006). However, the lengthened growing season would contribute to an increase in forest productivity in many regions, whereas the warmer and drier conditions are partly responsible for reduced forest productivity and increased forest fires in North America and Mediterranean basins (IPCC 2012).

By contrast, the decreasing MAT in the cooling period would exhibit asymmetrical features with obvious cooling in the northern hemisphere and slight cooling in the southern hemisphere (Xin et al. 2013). The MAP variation would be relatively minor with regional features. Terrestrial NPP is projected to globally increase slightly in this period. The cooling effect would be sufficiently strong to reduce the NPP of semi-desert, steppe, savanna, and tropical forest, as well as to restrain the increasing rates of warm desert and temperate forest. By contrast, the NPP of tundra & alpine steppe, cold desert, temperate humid grassland, and subtropical forest would increase. Terrestrial NPP in the TRZ and the STZ would diminish in this period. However, terrestrial NPP in the NTZ and NFZ is projected to continuously increase at a slower rate. Therefore, ecosystems in the TRZ would respond more directly and evidently to climate change compared to others. The consistent increasing trend of NPP in the NTZ is probably due to the largely distributed temperate forest area. In the STZ, the slowly increasing terrestrial NPP in this period can be attributed to the slight cooling effect because of the vast ocean area.

Conclusions

The consistent rise in temperature and redistribution of rainfall pattern would continue to affect natural biological systems. Under the RCP2.6 scenario, the terrestrial NPP is projected to increase from 127.04 ± 1.74 Pg DW·a^{-1} in 2030s to 127.62 ± 2.57 Pg DW·a^{-1} in 2070s. Temperate forest, the largest distributed vegetation, would contribute the most to the overall increasing trend, which may account for the combined effects of lengthening growing seasons and area expansions. The NPP of warm desert, savanna, and tropical forest is also projected to increase during this century, and would reach their peaks in 2050s. By contrast, the NPP of all the other vegetations is projected to decrease, even with a moderate increase from 2050s to 2070s. The global pattern of NPP dynamics would similarly occur in the TRZ. In the NTZ and NFZ, terrestrial NPP is projected to increase continually with a lower rate in the latter half of this century. However, the NPP of vegetation in high latitudes, such as tundra & alpine steppe, would diminish. By contrast, the NPP is projected to decrease continually in the STZ over the future decades. In general, terrestrial NPP would present an increasing–decreasing trend in response to the warming–cooling trend under the RCP2.6 scenario. However, it would fail to

recover to the state in the near future, such that ecosystems in the mid/high latitudes or elevation would continue to be the most vulnerable to climate change.

Acknowledgments This work was supported by the "APN Global Change Fund Project (No. ARCP2013-16NMY-LI)", "the Natural Science Foundation of Northwest A & F University (Z109021502)", "the National Natural Science Foundation of China (No. 41201178)", "The Key Project of Chinese National Programs for Fundamental Research and Development (973 Program, No. 2010CB950702)". We thank Prof. Jizhou Ren from Lanzhou University, Prof. Jiaguo Qi from the Michigan State University, Prof. Jingming Chen from the University of Toronto, Prof. Pavel Y. Groisman from the NOAA National Climatic Data Center for their guidance on the method and writing of this paper. We also appreciate the International Center for Tropical Agriculture (CIAT) for sharing datasets.

References

Alo CA, Wang G (2008) Potential future changes of the terrestrial ecosystem based on climate projections by eight general circulation models. J Geophys Res 113:G01004

Anav A, Mariotti A (2011) Sensitivity of natural vegetation to climate change in the Euro-Mediterranean area. Climate Res 46:277

Brzeziecki B, Kienast F, Wildi O (1995) Modelling potential impacts of climate change on the spatial distribution of zonal forest communities in Switzerland. J Veg Sci 6:257–268

Canadell JG, Pataki DE, Pitelka LF (2006) Terrestrial ecosystems in a changing world. Springer, German

Cao MK, Woodward FI (1998) Dynamic responses of terrestrial ecosystem carbon cycling to global climate change. Nature 393:249–252

Cao MK, Yu GR, Liu JY, Li KR (2005) Multi-scale observation and cross-scale mechanistic modeling on terrestrial ecosystem carbon cycle. Sci China Ser D 48:17–32

Cramer W, Friend AD, Kucharik C, Lomas MR, Ramankutty N, Sitch S, Smith B, White A, Young Molling C, Bondeau A, Woodward FI, Prentice IC, Betts RA, Brovkin V, Cox PM, Fisher V, Foley JA (2001) Global response of terrestrial ecosystem structure and function to CO_2 and climate change: results from six dynamic global vegetation models. Global Change Biol 7:357–373

Foley JA, Levis S, Costa MH, Cramer W, Pollard D (2000) Incorporating dynamic vegetation cover within global climate models. Ecol Appl 10:1620–1632

Gang C, Zhou W, Li J, Chen Y, Mu S, Ren J, Chen J, Pavel Ya G (2013) Assessing the spatiotemporal variation in distribution, extent and NPP of terrestrial ecosystems in response to climate change from 1911 to 2000. PLoS ONE 8:e80394

Gao Y, Zhou X, Wang Q, Wang C, Zhan Z, Chen L, Yan J, Qu R (2013) Vegetation net primary productivity and its response to climate change during 2001–2008 in the Tibetan Plateau. Sci Total Environ 444:356–362

Gonzalez P, Neilson RP, Lenihan JM, Drapek RJ (2010) Global patterns in the vulnerability of ecosystems to vegetation shifts due to climate change. Global Ecol Biogeogr 19:755–768

Grimm NB, Chapin FS III, Bierwagen B, Gonzalez P, Groffman PM, Luo Y, Melton F, Nadelhoffer K, Pairis A, Raymond PA (2013) The impacts of climate change on ecosystem structure and function. Front Ecol Environ 11:474–482

Hickler T, Vohland K, Feehan J, Miller PA, Smith B, Costa L, Giesecke T, Fronzek S, Carter TR, Cramer W (2012) Projecting the future distribution of European potential natural vegetation zones with a generalized, tree species-based dynamic vegetation model. Global Ecol Biogeogr 21:50–63

Hijmans RJ, Cameron SE, Parra JL, Jones PG, Jarvis A (2005) Very high resolution interpolated climate surfaces for global land areas. Int J Climatol 25:1965–1978

Horion S, Cornet Y, Erpicum M, Tychon B (2013) Studying interactions between climate variability and vegetation dynamic using a phenology based approach. Int J Appl Earth Obs Geoinf 20:20–32

IPCC (2007) Climate change 2007: Impacts, Adaptation and Vulnerability, Contribution of Working Group II to the Fourth Assessment Report of the IPCC. Cambridge University Press, Cambridge, p 630

IPCC (2012) Managing the Risks of Extreme Events and Disasters to Advance Climate Change Adaptation. A Special Report of Working Groups I and II of the Intergovernmental Panel on Climate Change. Cambridge University Press, Cambridge, p 582

James R, Washington R (2013) Changes in African temperature and precipitation associated with degrees of global warming. Clim Change 117:859–872

Jiang H, Peng C, Apps MJ, Zhang Y, Woodard PM, Wang Z (1999) Modelling the net primary productivity of temperate forest ecosystems in China with a GAP model. Ecol Model 122:225–238

Joshi M, Sutton R, Lowe J, Frame D (2011) Projections of when temperature change would exceed 2 °C above pre-industrial levels. Nat Clim Change 1:407–412

Lenihan JM, Drapek R, Bachelet D, Neilson RP (2003) Climate change effects on vegetation distribution, carbon, and fire in California. Ecol Appl 13:1667–1681

Lewis SL, Lopez-Gonzalez G, Sonké B, Affum-Baffoe K, Baker TR, Ojo LO, Phillips OL, Reitsma JM, White L, Comiskey JA (2009) Increasing carbon storage in intact African tropical forests. Nature 457:1003–1006

Liang TG, Feng QS, Cao JJ, Xie HJ, Lin HL, Zhao J, Ren JZ (2012) Changes in global potential vegetation distributions from 1911 to 2000 as simulated by the Comprehensive Sequential Classification System approach. Chin Sci Bull 57:1298–1310

Lieth H. 1977. Modeling the primary productivity of the world. In: Primary productivity of the biosphere., Springer, New York

Lieth H, Eas B (1972) Evapotranspiration and primary productivity: C.W. Thornthwaite memorial model. Publ Climatol 25:37–46

Lucht W, Schaphoff S, Erbrecht T, Heyder U, Cramer W (2006) Terrestrial vegetation redistribution and carbon balance under climate change. Carbon Balance Manag 1:6

Marshall DJ, McQuaid CD, Wouldiams GA (2010) Non-climatic thermal adaptation: implications for species' responses to climate warming. Biol Lett 6:669–673

Massot M, Clobert J, FerriERe R (2008) Climate warming, dispersal inhibition and extinction risk. Global Change Biol 14:461–469

McGuire AD, Melillo JM, Kicklighter DW, Joyce LA (1995) Equilibrium responses of soil carbon to climate change: Empirical and process-based estimates. J Biogeogr 22:785–796

McMahon SM, Parker GG, Miller DR (2010) Evidence for a recent increase in forest growth. Proc Natl Acad Sci 107:3611–3615

Melillo JM, Mcguire AD, Kicklighter DW, Moore B, Vorosmarty CJ, Schloss A (1993) Global climate change and terrestrial net primary production. Nature 363:234–240

Menzel A, Fabian P (1999) Growing season extended in Europe. Nature 397:659

Motew M, Kucharik CJ (2013) Climate induced changes in biome distribution, NPP and hydrology for potential vegetation of the Upper Midwest U.S.: A case study for potential vegetation. J Geophys Res 118:248–264

Nemani RR, Keeling CD, Hashimoto H, Jolly WM, Piper SC, Tucker CJ, Myneni RB, Running SW (2003) Climate-driven increases in

global terrestrial net primary production from 1982 to 1999. Science 300:1560–1563

Odum EP (1976) Fundamentals of ecology. W. B. Saunders, Philadelphia

Olson RJ, Scurlock J, Prince SD, Zheng DL, Johnson KR (2012) NPP Multi-Biome: global primary production data initiative products, R2. Data set. Available on-line [http://daac.ornl.gov] from the Oak Ridge National Laboratory Distributed Active Archive Center, Oak Ridge, Tennessee, USA

Parton WJ, Scurlock J, Ojima DS, Gilmanov TG, Scholes RJ, Schimel DS, Kirchner T, Menaut JC, Seastedt T, Garcia Moya E (1993) Observations and modeling of biomass and soil organic matter dynamics for the grassland biome worldwide. Global Biogeochem Cycles 7:785–809

Parton WJ, Scurlock J, Ojima DS, Schimel DS, Hall DO (1995) Impact of climate change on grassland production and soil carbon worldwide. Global Change Biol 1:13–22

Pearson RG, Dawson TP (2003) Predicting the impacts of climate change on the distribution of species: are bioclimate envelope models useful? Global Ecol Biogeogr 12:361–371

Piao S, Ciais P, Lomas M, Beer C, Liu H, Fang J, Friedlingstein P, Huang Y, Muraoka H, Son Y (2011) Contribution of climate change and rising CO_2 to terrestrial carbon balance in East Asia: a multi-model analysis. Global Planet Change 75:133–142

Potter CS, Randerson JT, Matson PA, Vitousek HA, Mooney HA, Klooster SA (1993) Terrestrial ecosystem production-A process model-based on global satellite and surface data. Global Biogeochem Cycles 7:811–841

Prince SD (1991) A model of regional primary production for use with coarse resolution satellite data. Int J Remote Sens 12:1313–1330

Ramirez-Villegas J, Jarvis A (2010) Downscaling global circulation model outputs: the delta method decision and policy analysis Working Paper No. 1. Policy Analysis 1: 1–18

Ren JZ, Hu ZZ, Zhao J, Zhang DG, Hou FJ, Lin HL, Mu XD (2008) A grassland classification system and its application in China. Rangeland J 30:199–209

Ren J, Liang T, Lin H, Feng Q, Huang X, Hou F, Zou D, Wang C (2011a) Study on grassland's responses to global climate change and its carbon sequestration potentials. Acta Prataculturae Sinica 20:1–22

Ren W, Tian H, Tao B, Chappelka A, Sun G, Lu C, Liu M, Chen G, Xu X (2011b) Impacts of tropospheric ozone and climate change on net primary productivity and net carbon exchange of China's forest ecosystems. Global Ecol Biogeogr 20:391–406

Roy J, Saugier B, Mooney HA (2001) Terrestrial global productivity. Academic Press, San Diego

Running SW, Hunt ER (1993) Generalization of a forest ecosystem process model for other biomes, BIOME-BGC, and an application for global-scale models. Scaling physiological processes: Leaf to globe: 141–158

Uchijima Z, Seino H (1985) Agroclimatic evaluation of net primary productivity of natural vegetation. 1. Chikugo model for evaluating net primary productivity. J Meteorol Soc Jpn 40:343–352

Van Vuuren DP, Edmonds J, Kainuma M, Riahi K, Thomson A, Hibbard K, Hurtt GC, Kram T, Krey V, Lamarque J (2011a) The representative concentration pathways: an overview. Clim Change 109:5–31

Van Vuuren DP, Stehfest E, Elzen MGJ, Kram T, Vliet J, Deetman S, Isaac M, Klein Goldewijk K, Hof A, Mendoza Beltran A, Oostenrijk R, Ruijven B (2011b) RCP2.6: exploring the possibility to keep global mean temperature increase below 2 °C. Clim Change 109:95–116

Wang W, Hashimoto H, Ganguly S, Votava P, Nemani RR, Myneni RB. (2010). Characterizing uncertainties in recent trends of global terrestrial net primary production through ensemble modeling. American Geophysical Union, Fall Meeting 1: 3

Woodward FI (1987) Climate and plant distribution. Cambridge University Press, Cambridge

Xin X, Cheng Y, Wang F, Wu T, Zhang J (2013) Asymmetry of surface climate change under RCP2. 6 projections from the CMIP5 models. Adv Atmos Sci 30:796–805

Xu Y, Zhao Z, Luo Y, Gao X (2005) Climate change projections for the 21st century by the NCC/IAP T63 Model with SRES scenarios. Acta Meteorologica Sinica 19:407

Yue TX, Fan ZM, Chen CF, Sun XF, Li BL (2011) Surface modelling of global terrestrial ecosystems under three climate change scenarios. Ecol Model 222:2342–2361

Zhang XS (1993) A vegetation-climate classification system for global change studies in China. Quat Sci 2:157–269

Zhang GG, Kang YM, Han GD, Sakurai K (2011) Effect of climate change over the past half century on the distribution, extent and NPP of ecosystems of Inner Mongolia. Global Change Biol 17:377–389

Zhang L, Ding Y, Wu T, Xin X, Zhang Y, Xu Y (2013) The 21st century annual mean surface air temperature change and the 2 °C warming threshold over the globe and China as projected by the CMIP5 models. Acta meteorologica Sinica 71:1047–1060

Zhou GS, Zheng YR, Chen SQ (1998) NPP model of natural vegetation and its application in China. Scientia Silvae Sinicae 34:2–11

Zhu WQ, Chen YH, Xu D, Li J (2005) Advances in terrestrial net primary productivity (NPP) estimation models. Chinese J Ecol 24:296–300